© 2017. Published by The Company of Biologists Ltd | Development (2017) 144, 4148-4158 doi:10.1242/dev.149914

RESEARCH ARTICLE

Talin regulates integrin β1-dependent and -independent cell functions in ureteric bud development

Sijo Mathew[1,*], Riya J. Palamuttam[1,*], Glenda Mernaugh[1], Harini Ramalingam[2], Zhenwei Lu[3,4], Ming-Zhi Zhang[1], Shuta Ishibe[5], David R. Critchley[6], Reinhard Fässler[7], Ambra Pozzi[1,4,8], Charles R. Sanders[9,3], Thomas J. Carroll[2] and Roy Zent[1,10,8,‡]

ABSTRACT

Kidney collecting system development requires integrin-dependent cell-extracellular matrix interactions. Integrins are heterodimeric transmembrane receptors consisting of α and β subunits; crucial integrins in the kidney collecting system express the β1 subunit. The β1 cytoplasmic tail has two NPxY motifs that mediate functions by binding to cytoplasmic signaling and scaffolding molecules. Talins, scaffolding proteins that bind to the membrane proximal NPxY motif, are proposed to activate integrins and to link them to the actin cytoskeleton. We have defined the role of talin binding to the β1 proximal NPxY motif in the developing kidney collecting system in mice that selectively express a Y-to-A mutation in this motif. The mice developed a hypoplastic dysplastic collecting system. Collecting duct cells expressing this mutation had moderate abnormalities in cell adhesion, migration, proliferation and growth factor-dependent signaling. In contrast, mice lacking talins in the developing ureteric bud developed kidney agenesis and collecting duct cells had severe cytoskeletal, adhesion and polarity defects. Thus, talins are essential for kidney collecting duct development through mechanisms that extend beyond those requiring binding to the β1 integrin subunit NPxY motif.

KEY WORDS: Kidney, Signaling, Nuclear magnetic resonance, Tubules

INTRODUCTION

The kidney consists of numerous nephrons that drain into the multibranched collecting system. Embryologically, the nephrons are derived from the metanephric mesenchyme, while the collecting system is formed by iterative branching of the ureteric bud (UB), a process regulated by multiple factors, including integrin-dependent cell-extracellular matrix (ECM) interactions (Mathew et al., 2012a).

[1]Division of Nephrology and Hypertension, Department of Medicine, Vanderbilt University Medical Center, Nashville, TN 37232, USA. [2]Department of Medicine and Department of Molecular Biology, University of Texas Southwestern Medical Center, Dallas, TX 75390, USA. [3]Center for Structure Biology, Vanderbilt University Medical Center, Nashville, TN 37232, USA. [4]Department of Molecular Physiology, Vanderbilt University Medical Center, Nashville, TN 37232, USA. [5]Department of Internal Medicine, Yale University School of Medicine, New Haven, CT 06510, USA. [6]Department of Biochemistry, University of Leicester, Leicester LE1 7RH, UK. [7]Department of Molecular Medicine, Max Planck Institute of Biochemistry, Martinsried 82152, Germany. [8]Veteran Affairs Hospital Nashville, TN 37212, USA. [9]Department of Biochemistry, Vanderbilt University Medical Center, Nashville, TN 37232, USA. [10]Department of Cell and Developmental Biology, Vanderbilt University Medical Center, Nashville, TN 37232, USA.
*These authors contributed equally to this work

‡Author for correspondence (roy.zent@vanderbilt.edu)

C.R.S., 0000-0003-2046-2862; R.Z., 0000-0003-2983-8133

Received 1 February 2017; Accepted 28 September 2017

Integrins, transmembrane receptors that mediate ECM interactions, are essential for multiple cell functions. There are 24 integrins composed of αβ heterodimers (Pozzi and Zent, 2013). Among the eight β subunits, integrin β1 is most abundantly expressed and pairs with 12 α subunits, including laminin- (α3, α6) and collagen- (α1, α2) binding subunits, thereby forming the principal integrins expressed by the kidney (Mathew et al., 2012a). Integrin β1 is required for normal kidney collecting system development and its selective deletion in the UB (E10.5) causes a severe branching morphogenesis defect (Zhang et al., 2009).

The integrin β1 cytoplasmic tail contains two well-defined NPxY motifs (Y783 at the membrane proximal and Y795 at the membrane distal sites) (Czuchra et al., 2006). The functional significance of these domains was addressed by mutagenesis studies where both Y783 and Y795 were mutated to alanine (YY/AA). YY/AA mutations selectively induced in the skin epidermis showed the same abnormalities as mice lacking the β1 subunit; however, mice carrying the single β1 Y783A mutation exhibited only minor defects (Meves et al., 2011). In contrast, mice carrying the YY/AA mutations in the developing UB displayed a significantly less severe phenotype than mice lacking the β1 subunit (Mathew et al., 2012b). The effect of the β1 Y783A mutation in the UB is unknown.

The β1 tail NPxY motifs bind crucial cytosolic proteins, with talins representing the most studied (Ye et al., 2014). There are two talin isoforms in mammals, talin 1 and talin 2, which have the same domain structure and 76% amino acid identity. In some tissues, these isoforms are differentially expressed, whereas in others, such as the kidney collecting system, both are expressed (Praekelt et al., 2012). Talins are required for integrin activation and they provide a direct link between integrins and the actin cytoskeleton by acting as a scaffold for the recruitment of other proteins, such as vinculin and actin (Albiges-Rizo et al., 2009; Calderwood et al., 2013). Talins are thought to induce integrin activation by first binding to the membrane-proximal NPxY of the β integrin tail after which they interact with a more membrane proximal binding site to destabilize the putative integrin salt bridge and then stabilize the helical structure of the membrane proximal region of the β1 integrin tail (Wegener et al., 2007). Talins are required for normal development and constitutive deletion of talin 1 causes E8.5 lethality due to gastrulation defects (Monkley et al., 2000). Talin 1 was also shown to be required for integrin αIIbβ3 activation (Calderwood et al., 1999), and platelet aggregation and clotting (Nieswandt et al., 2007; Petrich et al., 2007b). Talin 1 is important for the normal function of podocytes in the glomeruli of the kidneys, where it regulates the actin cytoskeleton rather than integrin activation (Tian et al., 2014). Talin 2 is more dispensable than talin 1. Global talin 2-null mice are viable with only a mild muscle phenotype (Debrand et al., 2012). Both talins are required for normal muscle development. Mice lacking both isoforms in muscle have a fatal perinatal phenotype,

Development (2017) 144, 4148-4158 doi:10.1242/dev.149914

which was not because muscle cells cannot activate their integrins but due to their inability to generate force across integrins (Conti et al., 2008, 2009; Manso et al., 2013).

The kidney tubules, including the collecting ducts (CDs), have very high levels of talin 1 and talin 2 (Praekelt et al., 2012); however, their importance in development is unknown. In this study, we have defined the function of talins and the role of talin binding to the β1 integrin subunit in UB development.

RESULTS

Disrupting the NPxY talin binding site on integrin β1 leads to defective UB development

To define the role of β1 integrin-talin interactions in UB development, we generated mice that selectively carry the Y783A substitution (Czuchra et al., 2006) in the developing UB. Mice expressing the Y/A mutation were bred by intercrossing heterozygous Y/A mutant mice with floxed β1 integrin mice and transgenic mice expressing Cre recombinase under the hoxB7 promoter (Yu et al., 2002). The offspring had deletion of the floxed β1 allele starting at E10.5 in the UB and expressed only the Y/A mutant allele. Y/A mutant mice were born in a normal Mendelian ratio, but at 3 weeks of age, they were significantly smaller than wild-type controls (4.9±0.8 versus 9.95±0.54 g, $P<0.05$), and at 6 months they were sacrificed due to failure to thrive. The phenotype was equally penetrant in both male and female mice. The kidneys of 4-week-old Y783A mice were significantly smaller than in wild-type mice (Fig. 1A-F) and ∼20% of the medullary and cortical collecting ducts were dilated. By 3 months there was increased cellularity and destruction of epithelia within the collecting ducts (Fig. 1G,J) and by 6 months the mice developed hypercellularity and fibrosis, resulting in an end-stage kidney (Fig. 1H,I). High-powered microscopy of the medulla of the kidneys after staining with either *Dolichos biflorus*, which stains the CDs and antibodies directed against Tamm-Horsfall protein (which stains the thick ascending limb of the loop of Henle), revealed that the dilated tubules with increased cellularity were CDs (Fig. 1K,L).

The adult phenotype of the Y783A mice was consistent with defects in development. We therefore determined when this became identifiable by characterizing mutant kidneys at E12.5, E15.5 and E17.5 (Fig. 2A-F). At E12.5, the size of the wild-type and Y783A mouse embryos was similar (798±4 mm versus 796±8 mm) as were the kidneys. Hematoxylin and Eosin-stained E12.5 kidneys suggested the mutant UB had undergone less branching morphogenesis than the wild-type mice. This early branching defect was verified by performing Wnt11 *in situ* hybridization on whole-mount kidneys at E12.5. Whereas wild-type kidneys had undergone several rounds of branching, all Y783A kidneys analyzed ($n=6$) appeared to be arrested at the T-bud stage (Fig. 2C,D). At E15.5, branching morphogenesis had progressed, although the Y783A kidneys were still significantly smaller than wild type with fewer collecting ducts visible (Fig. 2E-F). At E17.5, the differences in kidney size between wild type and Y783A mutants were even more obvious (Fig. 2G-H) with fewer dilated collecting ducts present (Fig. 2I,J).

Owing to the branching morphogenesis phenotype in the Y783A kidney, we investigated the defects at E15.5 in more detail. Although the size of the Y783A and wild-type mice was not significantly different (990±17 mm versus 883±28 mm), the Y783A kidneys were significantly smaller (Fig. 3A-C). When we quantified the number of UB tips in intact whole-mount kidneys stained with antibodies against E-cadherin and imaged by confocal microscopy (Fig. 3D-H) (Movies 1 and 2), there were ∼50% fewer UB tips in the Y783A mice (Fig. 3D,E,H). UB morphology was also abnormal in the mutants. UB tips were broader and misshapen compared with wild type (Fig. 3F,G). Although these studies demonstrated a significant difference in branching between mutant

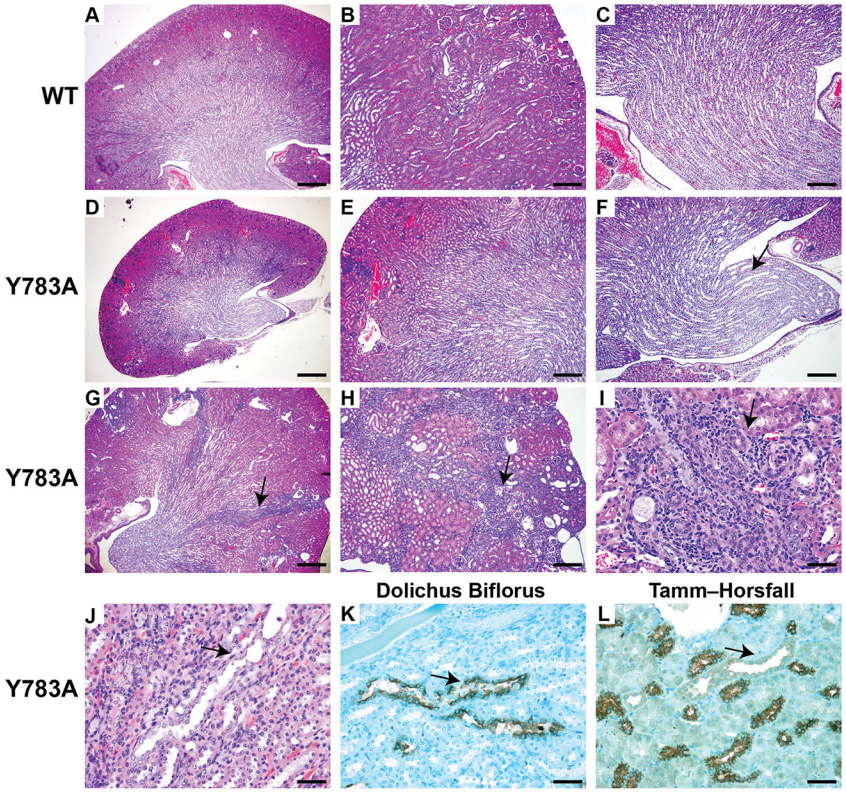

Fig. 1. Integrin β1 Y783A kidneys are small and fibrotic. (A-C) Periodic acid-Schiff (PAS)-stained kidney slides of the whole kidney (A), the cortex (B) and medulla (C) of 4-week-old wild-type ($β1^{flox/flox}$) kidneys. Scale bars: 500 µm in A; 200 µm in B,C. (D-I) PAS-stained slides of the Y783A kidneys. Four-week-old Y783A kidneys are smaller (D), with a smaller cortex (E) and a hypoplastic dysplastic medulla and papilla (arrow) (F). Scale bars: 500 µm in D; 200 µm in E,F. By 3 months of age, the Y783A kidneys have fibrosis in the medulla and medullary rays (arrow) (G). Scale bar: 200 µm. By 5 months of age, the Y783A mice have disorganized, hypercellular and fibrosed tubules (arrows) in the medulla and medullary rays (H,I). Scale bars: 100 µm. (J) The CDs (arrow) of 3-month-old kidneys display evidence of dilatation and intratubular cell proliferation. Scale bar: 50 µm. (K,L) The tubule (arrow) was verified to be CD by staining positive for the lectin *Dolichos biflorus* (K) and negative for Tamm-Horsfall protein which stain the thick ascending limb (L). Scale bars: 50 µm. At least six male or female mice for each of the time points was examined.

Development (2017) 144, 4148-4158 doi:10.1242/dev.149914

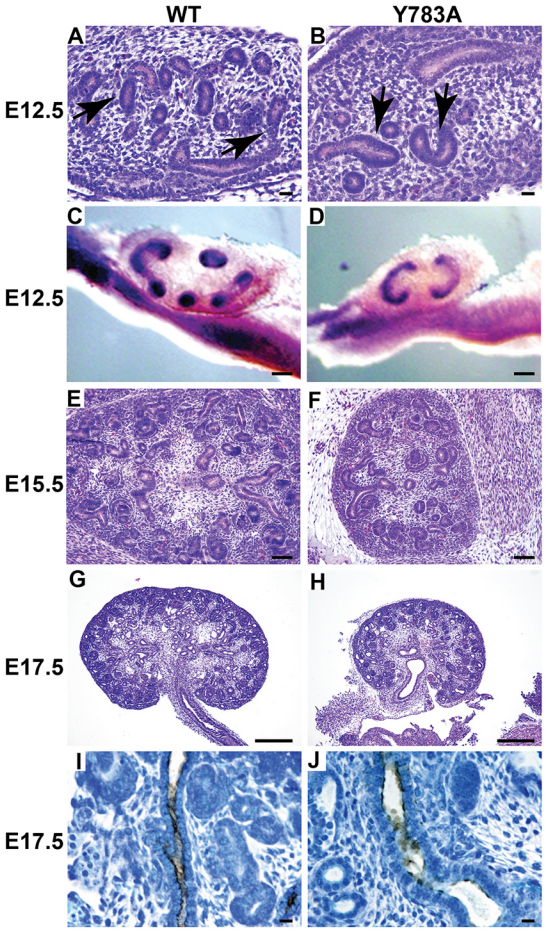

Fig. 2. Integrin β1 Y783A kidneys are small with evidence of abnormal UB development. (A-F) Kidneys were isolated from embryos of wild-type and Y783A mice at E12.5 (A-D). The branching UB is indicated with arrows (A,B). Scale bar: 50 µm. *In situ* hybridization of whole-mount kidneys were performed with antisense to Wnt11 (C,D). Scale bars: 100 µm. Y785A kidneys at E15.5 (E,F) and E17.5 (G,H) were small and had less UB branching. Scale bars: 100 µm in E,F; 200 µm in G,H. (I,J) The CDs designated by staining positive for the lectin *Dolichos biflorus* were dilated in E17.5 kidneys. Scale bars: 50 µm. At least six embryos at each time point were examined.

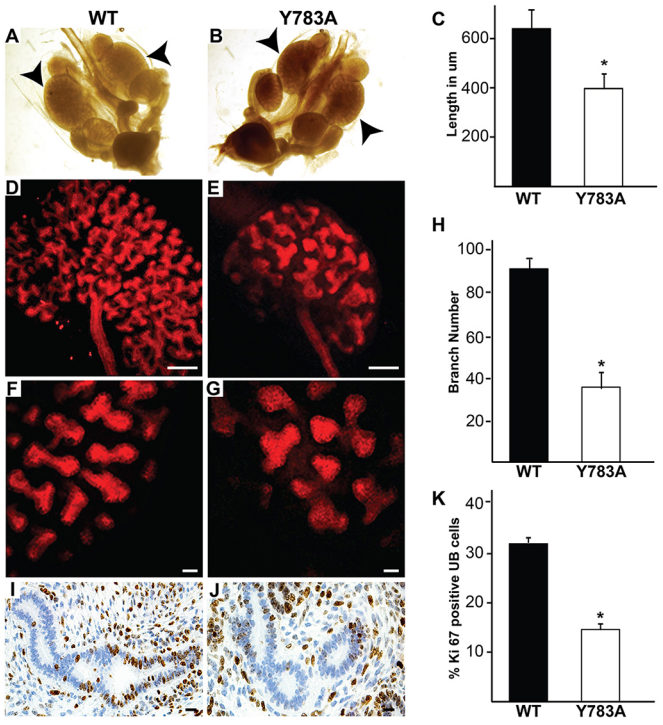

Fig. 3. Integrin β1 Y783A kidneys have a branching morphogenesis defect. (A-C) Whole-mount dissections of the urogenital tract reveal that the length of the E15.5 Y783A kidneys was significantly less than in wild-type mice. (D-H) Whole mounts of E15.5 kidneys, stained with E-cadherin and imaged with confocal microscopy show a significant branching defect. At least six mice of each genotype were examined. Scale bars: 100 µm in D-G. (I,J) High-powered images of Ki67 staining in E15.5 Y783A and wild-type mice showed decreased UB cell proliferation in Y783A mice at E15.5. Scale bars: 100 µm. (K) The number of Ki67-positive cells was quantified and expressed as the mean±s.d. of five high-power fields in five mice. **P*<0.05 (between wild-type and Y783A mutant mice).

and wild-type kidneys of mice from the same litters, they do not assess absolute branch number within the developing UB. When we examined cell proliferation and apoptosis, no difference in apoptosis (as assessed by TUNEL staining) was present (data not shown). There was, however, a significant decrease in the overall number of Ki67-positive UB cells in the Y783A mutants at E15.5 (15% versus 34%, $P<0.05$, Fig. 3I-K). As most proliferation occurs in the UB tips, these data suggest that decreased cell proliferation is at least in part responsible for the branching phenotype in the Y783A mutants. Thus, we conclude that Y783 of the membrane-proximal NPxY motif of the β1 integrin subunit regulates UB branching morphogenesis.

The membrane-proximal NPxY of integrin β1 regulates CD cell function

We generated CD cells expressing the Y783A mutant to identify the cellular mechanisms underlying the *in vivo* development phenotypes. β1-null CD cells were transfected with either β1-WT or β1-Y783A mutant human cDNA and flow sorted for equal levels of expression (data not shown) (Mathew et al., 2012b). Y783A and wild-type CD cells spread equally and looked identical when grown on glass coverslips with 10% serum (Fig. 4A). When the Y783A CD cells were placed in 3D collagen/matrigel gels, they did not form tubules and grew as cysts (Fig. 4C,D). We next defined which crucial cell functions required for tubulogenesis were affected by the Y783A mutation by performing cell-adhesion, migration and proliferation assays on collagen I and laminin-511 (a major component of the kidney tubular basement membranes) (Fig. 4E-G). Y783A mutant cell adhesion (Fig. 4E) and migration (Fig. 4F) were decreased by about 75% and 50% on collagen I and Ln-511, respectively. By contrast, Y783A cell proliferation was reduced by only ∼25% on each of these substrates (Fig. 4G). Thus, the Y783A mutation did not alter CD cell morphology under normal culture conditions but CD cells are unable to undergo 3-D tubulogenesis. This was primarily caused by decreased cell adhesion and migration, and to a lesser extent by reduced proliferation on β1 integrin-dependent substrates.

The membrane-proximal NPxY of integrin β1 regulates CD cell signaling

A key requirement for cell adhesion is the ability of activated integrins to bind their ligands. We assessed this by determining the binding of antibody 12G10 (which binds to active integrins) relative to an antibody that binds integrins irrespective of their conformation (Mould et al., 1995). The integrin activation index of Y783A CD cells was approximately half of the wild-type cells (Fig. 5A). When signaling pathways activated following integrin-dependent cell

Development (2017) 144, 4148-4158 doi:10.1242/dev.149914

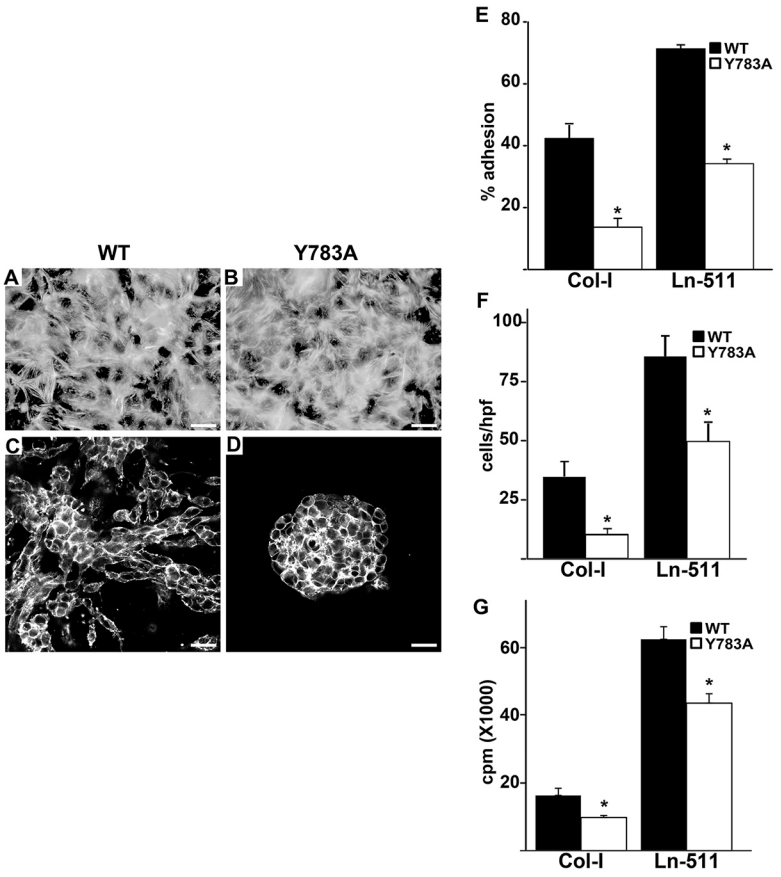

Fig. 4. Y783A mutations in the β1-integrin tail alter integrin-dependent cell functions. (A,B) Wild-type and Y783A mutant CD cells grown on plastic in the presence of 10% FBS, stained with rhodamine-phalloidin and visualized by immunofluorescent microscopy. Scale bars: 50 µm. (C,D) Wild-type and Y783A mutant CD cells placed in 3D collagen I/Matrigel gels for 7 days in the presence of 5% FBS, stained with rhodamine-phalloidin and visualized by confocal microscopy. Scale bars: 50 µm. (E) CD cell populations were allowed to adhere to collagen I (Col-1) or laminin 511 (Ln-511) for 1 h. Data are mean±s.d. of three experiments in triplicate. *P<0.05 (between wild type and mutant). (F) CD cells were plated on transwells coated with Col-1 or Ln-511, and migration, measured as cells per high powered field (hpf), was evaluated after 4 h. Data are mean±s.d. of three experiments in triplicate. *P<0.05 (between wild type and mutant). (G) CD cell populations were plated on collagen I (Col-1) or laminin 511 (Ln-511). After 24 h, the cells were treated with [3H] thymidine and incubated for a further 24 h. [3H] thymidine incorporation (in cpm) was then determined. Data are mean±s.d. of three experiments in triplicate. *P<0.05 (between wild type and Y785A integrins).

adhesion on Ln-511 were assessed, there was no difference in FAK (Fig. 5B,C) or Erk (Fig. 5D,E) activation between the cells, although there was a significant decrease in Akt (Fig. 5F,G) activation in the Y783A mutants. Thus, the Y783A mutation decreased β1 integrin binding to the affinity-dependent 12G10 antibody and adhesion-dependent Akt activation, but did not alter FAK and Erk signaling.

Glial cell line-derived neurotrophic factor (GDNF) is crucial for the initiation of UB development and fibroblast growth factors (FGFs) play a major role in later UB branching morphogenesis (Dressler, 2006). As downstream signaling of both these factors in CD cells is dependent on integrin β1 (Zhang et al., 2009), we investigated whether this is reliant on the membrane proximal NPxY. We treated wild-type or Y783A CD cells adherent on laminin-511 with either GDNF (Fig. 5H-M) or FGF10 (Fig. 5N-S) and determined their signaling responses over time. In wild-type cells, FAK (Fig. 5H,I,N,O), Akt (Fig. 5J,K,P,Q) and Erk (Fig. 5L,M and Fig. 4R,S) phosphorylation was strongly induced by GDNF and FGF-10. Peak activation was at 15 min and was sustained to 45 min for FAK, but diminished over time for Akt and Erk. When the Y783A CD cells were stimulated with GDNF or FGF10, FAK was stimulated and sustained to the same level as in the wild-type CD cells (Fig. 5H,I,N,O). By contrast, the level and duration of Akt activation was significantly decreased in the Y783A CD cells after either GDNF or FGF10 stimulation (Fig. 5J,K,P,Q). Following GDNF stimulation, Erk activation was significantly less in the Y783A CD cells than in wild-type cells at all time points measured (Fig. 5L,M,R,S). Erk activation was similar in both Y783A and wild-type CD cells at 15 min following FGF10 stimulation; however, it was not sustained in the Y783A CD cells (Fig. 5L,M, R,S). These data indicate that the membrane proximal NPxY motif of the β1 integrin modulates the response of Akt and Erk, but not FAK signaling, in CD cells in response to GDNF and FGF10.

The membrane proximal NPxY motif is the principal talin-binding site of the integrin β1 cytoplasmic tail

The relatively mild phenotype resulting from the Y783A mutation was somewhat unexpected as this mutation is predicted to prevent interactions between integrin β1 and talins, which are crucial for integrin function (Calderwood et al., 1999; Monkley et al., 2000; Nieswandt et al., 2007; Petrich et al., 2007a,b). An explanation for this result is that sufficient interactions between talins and integrins occur for function. We therefore used nuclear magnetic resonance (NMR), a highly sensitive method that can define the affinities of protein binding in a phospholipid bilayer, to test how efficiently the Y783 mutation disrupted interactions with talins. Talins are composed of a rod domain coupled to a 'head' comprising an atypical FERM domain (with F0, F1 F2 and F3 subdomains) (Calderwood et al., 2013). NMR studies in aqueous buffers have demonstrated that the β1 cytoplasmic tail binds to the isolated talin F3 domain of talin 1 with a K_d of ∼500 µM but this affinity drops to∼5 mM as a consequence of the β1 Y783A mutation (Anthis et al., 2010). The isolated talin F3 domain of talin 1 has been shown to bind to the full-length transmembrane and cytoplasmic tail domains of β1 in bicelles with a K_d of ∼27 µM (Lu et al., 2016). In contrast, binding of the entire talin head (F0-F3) to the integrin β1 cytosolic domain exhibits an apparent K_d value of 124 nM, three orders of magnitude tighter than for F3 alone (Goult et al., 2010). Basic residues in the talin F2-F3 domain have been reported to associate with acidic phospholipids in the cell membrane to help mediate activation and clustering of integrin β3 (Anthis et al., 2009; Moore et al., 2012; Saltel et al., 2009).

Development (2017) 144, 4148-4158 doi:10.1242/dev.149914

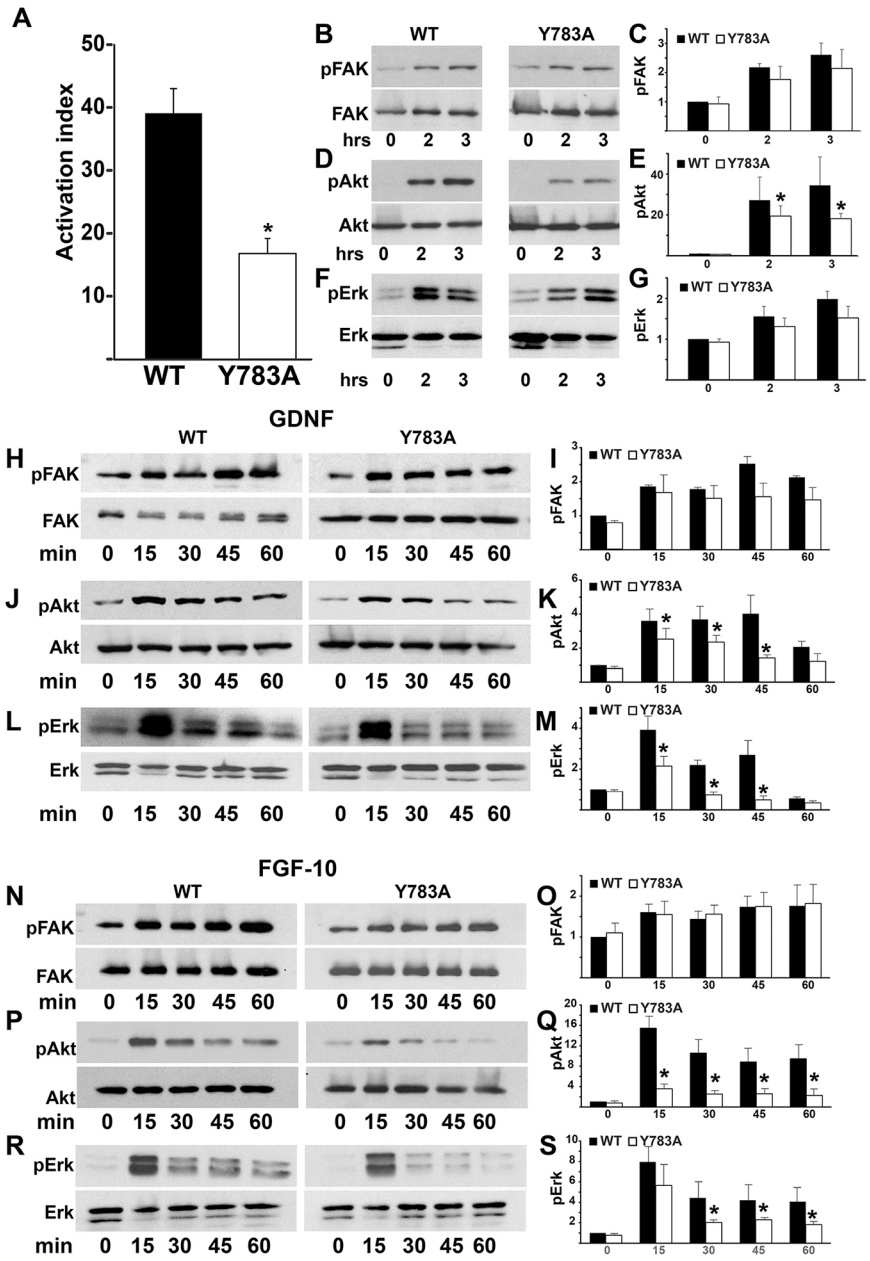

Fig. 5. Y783A mutations in the β1-integrin tail alter integrin-dependent activation and signaling. (A) The β1-integrin activation index was determined as described in the Materials and Methods. Data are mean ±s.d. of three experiments performed in triplicate. **P*<0.05 (between cells expressing wild-type and Y785A integrin). (B-G) Wild-type and Y783A CD cells were plated in serum-free medium on Ln-511. Cells were lysed and lysates were analyzed by western blotting for levels of phosphorylated and total FAK (B), Akt (D) and Erk1/2 (F). Phosphorylated protein levels were measured by densitometry using Image J and normalized to total protein. The fold changes in phosphorylated/total protein at different time points relative to the Y783A mutant at the '0' time point are shown in C,E,G. **P*<0.05 (between cells expressing wild-type and mutant integrins). (H-M) Wild-type and Y783A CD cells were allowed to adhere to Ln-511 for 1 h, after which they were treated with GDNF for the times indicated. The cells were then lysed and analyzed by western blotting for levels of phosphorylated and total FAK (H), Akt (J) and Erk1/2 (L). Levels of phosphorylated proteins were measured by densitometry and normalized to total protein, as indicated above. Data are mean±s.d. of five experiments. **P*<0.05 (between wild-type and mutant integrins). (N-S) Wild-type and Y783A CD cells were allowed to adhere to Ln-511 for 1 h, after which they were treated with FGF for the times indicated. Cell lysates were analyzed for levels of phosphorylated and total FAK (N), Akt (P) and ERK1/2 (R). Levels of phosphorylated proteins were measured by densitometry and normalized to total protein, as indicated above. **P*<0.05 between cells expressing wild-type and mutant integrins (O,Q,S).

Based on studies showing that the full talin 1 head domain (F0-F3) is needed for integrin β1 activation (Bouaouina et al., 2008), we examined binding of this domain (1-433 amino acids, 55 kDa) to the combined transmembrane/cytoplasmic domain (TM/CTD) of integrin β1 subunit in phospholipid bicelles (Fig. 6). Phospholipid bicelles provide an ideal model membrane that maintains the integrin TM domain in solution and ensures its native-like orientation relative to the attached cytosolic domain. Binding of the talin F0-F3 domain to the β1 TM/CTD results in gradual peak disappearance, characteristic of binding kinetics that are in the slow exchange NMR time scale regime (Fig. 6). The fact that binding appears to saturate when the F0-F3 domain: β1 TM/CTD ratio exceeds 1:3 suggests that β1 in bicelles is homotrimeric (Li et al., 2001) and it is only the first binding event in the process of 3:3 complex formation that is spectroscopically detectable. The fact that a new set of peaks does not appear upon complex formation suggests that the complex formed between the homotrimeric integrin β1 in bicelles and a single subunit of the F0-F3 domain is so large that its NMR resonances are undetectably broad. Plots of reductions in peak intensities from β1 integrin Y783, V790 and V791 as a function of talin concentration were therefore fitted by a model for single-site binding (based on the assumption that one F0-F3 domain binds one integrin homotrimer) (Fig. 6B). The results indicate that K_d for the binding of F0-F3 to β1 TM/CTD is 1.9±1.2 μM (Fig. 6B). The binding affinity of the talin F0-F3 domain to the β1 Y783A mutant was greatly reduced. K_d could not be determined because binding was not saturated at the highest level of F0-F3 tested (Fig. 6C and Fig. S1), indicating that K_d>100 μM. This indicates that Y783 in the proximal NPxY motif of integrin β1 is critically involved in the association between these proteins in membrane-mimicking phospholipid bicelles, and there is virtually no interaction between talin and the Y783A mutant β1 cytoplasmic tail.

Development (2017) 144, 4148-4158 doi:10.1242/dev.149914

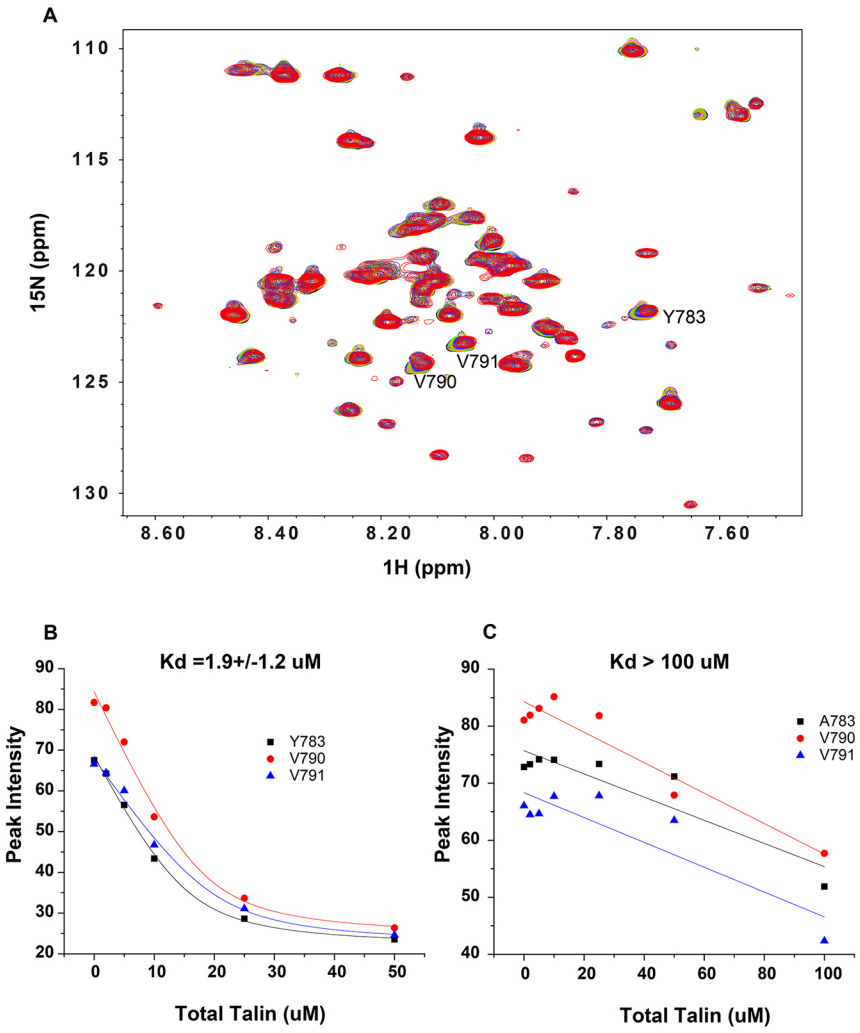

Fig. 6. Talin 1 head domain binding to integrin β1 in a bilayer environment is decreased by a mutation in the membrane-proximal NPxY motif of integrin β1. The unlabeled talin head domain (F0-F3) was titrated into a solution containing the 15N-labeled integrin β1 TM/CTD domain in D7PC/POPC/POPS bicelles (as described in the Materials and Methods). 1H,15N-TROSY NMR experiments were carried out. (A) Superimposed NMR spectra of 15N-labeled wild-type integrin β1 TM/CTD (0.2 mM) in the presence of different concentrations of unlabeled talin head domain (F0-F3): black (0 μM), pink (2 μM), green (5 μM), yellow (10 μM), blue (25 μM) and red (50 μM). Not shown is the spectrum for an additional titration point at 75 μM talin F0-F3, where the peaks disappeared completely, indicative of complete saturation to form a spectroscopically invisible complex. (B) Fit of talin head titration data using a 1:1 binding model (Eqn 1 in the Materials and Methods) for complex formation between the talin 1 head domain and wild-type 15N-labeled integrin β1 TM/CTD. Fits of the reductions in peak intensities are shown for integrin β1 TM/CTD amide peaks from sites Y783, V790 and V791 residues, yielding an average K_d of 1.9±1.2 μM. (C) Data for titration of the talin 1 head domain to 15N-labeled Y783A mutant integrin β1 TM/CTD. The NMR spectra from which these data were derived appear in Fig. S1. An attempt was made to analyze the data the same way as for the wild-type integrin β1 TM/CTD. However, statistically meaningful results could not be obtained because the data exhibit no curvature (indicating <50% saturation even at the highest talin concentration tested; 100 μM). This suggests that the K_d for complex formation between a single talin head domain with a single integrin β1 trimer is >100 μM.

Talin is crucial for kidney development

Our *in vivo* and *in vitro* data indicate that disrupting β1 binding to talins causes a moderate renal collecting system developmental phenotype. We therefore tested the hypothesis that ablating talins would phenocopy the Y783A mutation (Morse et al., 2014). Talins 1 and 2 are closely related, compensate for each other (Calderwood et al., 2013) and are highly expressed in the mouse collecting system (Praekelt et al., 2012). We deleted both isoforms in the UB by crossing the talin $1^{flox/flox}$ mouse (Conti et al., 2008) with the constitutive talin 2-null mouse (Debrand et al., 2012). These double homozygote mice were crossed with the hoxB7-cre mouse to delete talin 1 specifically in the UB. In contrast to the β1 Y783A mutant mice, there was 100% lethality of these mice and they were anephric at birth (Fig. 7A).

To determine the cause of the agenesis in the talin mutants, we performed *in situ* hybridization on isolated urogenital systems at E11 and 12.5 with a probe for Ret. Although a T-shaped UB structure was visible in the E11 wild-type urogenital system, the Talin mutants contained an unbranched UB (Fig. 7B-C). At E12.5, although the UB had branched several times in the wild-type mice, the mutant UB was halted at a T-shaped stage in all mutants assessed (Fig. 7D,E, n=4). The halted development was confirmed when the UB of E12.5 kidneys was stained with E-cadherin and confocal microscopy on whole mounts was performed (Fig. 7F-G) (Movies 3 and 4). This result suggests that talins are required for early UB branching that occurs soon after induction from the Wolffian duct.

Double talin-null CD cells have a major adhesion defect

To define the mechanisms underlying this unexpected phenotype, we derived CD cells from the talin $1^{flox/flox}$/talin 2-null mouse and deleted the talin 1 gene *in vitro* using adeno-Cre virus to produce talin 1/2 knockout (KO) CD cells. At least three clones were characterized and shown to have consistent cell behavior. Talin $1^{flox/flox}$/talin 2 null CD (wild-type) cells were used as controls as they behaved phenotypically like CD cells isolated from wild-type mice (data not shown). The talin 1/2 KO cells were round, never adhered to plastic and did not develop stress fibers, even when grown in the presence of 10% serum (Fig. 8A,B). Talin 1/2 knockout CD cells placed in 3D collagen-I/MG gels were unable to develop tubules and formed clumps of rounded cells that proliferated slowly (Fig. 8C,D). Expression of β1, α1, α2, α3 and α6 integrin subunits in talin 1/2 KO and wild-type CD cells were similar (data not shown). The severe adhesion defect precluded adhesion and migration assays on 2D substrates, but we could measure the β1 integrin activation index, which was about 25% of the control cells (Fig. 8E). We confirmed a severe proliferation defect in the talin 1/2 KO CD cells grown on LM-511 in the presence of 1% serum (Fig. 8F). Thus, deleting talin 1 and 2 in CD cells causes a severe defect in the ability of β1 integrins to bind ligand, as well as adhesion, spreading and proliferation abnormalities resulting in their inability to undergo tubulogenesis.

Development (2017) 144, 4148-4158 doi:10.1242/dev.149914

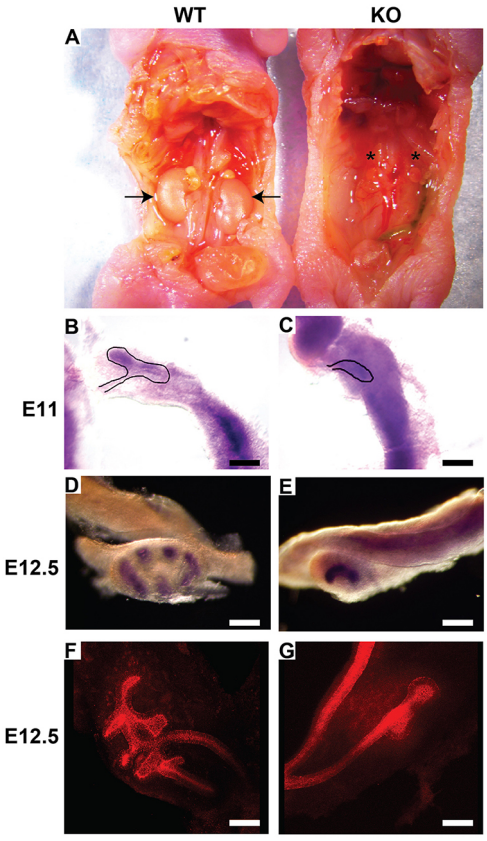

Fig. 7. Talin 1/2-null mice are anephric due to the arrest of UB growth at E12.5. (A) Newborn talin 1/2-null mice were anephric, despite normal localization of the adrenal gland (asterisks). The arrows in the wild-type mouse indicate the kidneys. Twenty mice were investigated with similar results. (B-E) *In situ* hybridization of Ret was performed on whole mounts of E11 and E 12.5 kidneys. Induction of the UB at E11 was delayed in the talin-null kidneys (B,C) and it never progressed beyond the T shape in the E12.5 kidneys (D,E). Scale bars: 100 µm. (F,G) Whole mounts of E12.5 kidneys from wild-type and talin 1/2-null mice were stained with E-cadherin and visualized by confocal microscopy. Scale bars: 100 µm. At least three embryos of each phenotype were investigated with similar results.

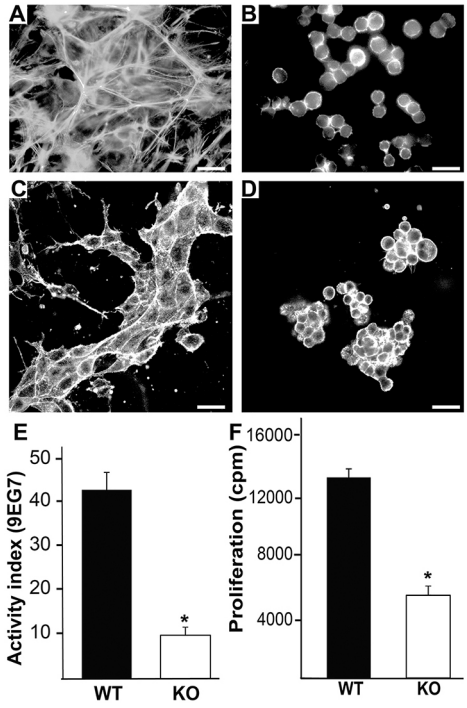

Fig. 8. Talin 1/2 KO CD cells have major spreading, tubulogenesis and proliferation defects. (A,B) Wild-type and talin 1/2 KO CD cells were grown in 10% FBS on plastic, stained with rhodamine-phalloidin and visualized by immunofluorescent microscopy. Scale bars: 50 µm. (C,D) Wild-type and talin 1/2 KO (KO) CD cells placed in 3D collagen and Matrigel gels for 7 days in the presence of 5% FBS were stained with rhodamine-phalloidin and visualized by confocal microscopy. Scale bars: 50 µm. (E) The activation index of the β1 integrin was determined as described in the Materials and Methods. Data are mean±s.d. of three experiments performed in triplicate. **P*<0.05 between wild-type and talin 1- and talin 2-null cells. (F) Thymidine incorporation in wild-type and talin 1/2 KO CD cells plated on Ln-511 in the presence of 10% FBS was measured as described in the Materials and Methods. Data are mean±s.d. of three experiments performed in triplicate. **P*<0.05 (between wild-type and talin 1/2 KO cells).

Talin-null CD cells have a major polarity defect

The phenotypical abnormalities of the talin1/2 KO CD cells suggested they have polarity abnormalities. When we grew wild-type and talin1/2 KO cells on transwells, the wild-type CD cells develop a polarized monolayer, whereas talin1/2 KO CD cells grew as non-confluent multilayered cell populations as seen in *z*-stacks and cross-sections of CD cells stained with rhodamine phalloidin (Fig. 9A-D). The amount of the tight junction protein ZO-1 was significantly reduced in the talin1/2KO CD cells (Fig. 9M) and it was found in punctate regions rather than the expected cell membrane staining (Fig. 9E-F). Similarly, there was much less E-cadherin, which was also not localized to the cell membrane (Fig. 9G-H). The talin 1/2 KO cells showed increased expression of the tight junction protein claudin 3, found within the cytoplasm and not localized to the membrane (Fig. 9I-K). There was increased expression of claudin 7 in the talin1/2 KO cells, which was poorly localized in punctate regions of the cell membrane (Fig. 9K-L). Thus, deleting talins 1 and 2 in CD cells causes major polarity defects that include alterations in expression and localization of adherens and tight junction proteins.

DISCUSSION

Binding of the talin head to the membrane proximal NPxY motif of the β1 integrin tail regulates integrin activation and function (Calderwood et al., 1999; Ginsberg, 2014; Moser et al., 2009; Nieswandt et al., 2007; Petrich et al., 2007a; Ye et al., 2014). In this study, we directly investigated the importance of the talin-β1 integrin NPxY motif interaction in UB development and CD duct cell tubulogenesis. We showed that introducing a β1 integrin Y783A mutation into the UB in mice and CD cells resulted in moderate UB branching morphogenesis and tubulogenesis defects, which were much less severe than when β1 integrin was deleted (Wu et al., 2009; Zhang et al., 2009). The Y783A mutation was shown to reduce the affinity for the talin 1 head by a factor of at least 50. However, co-deletion of the talins from the developing UB resulted in total absence of kidneys due to a major branching morphogenesis defect apparent at E12.5. In addition to severe abnormalities of integrin-dependent functions, talin null CD cells were unable to polarize normally and the actin cytoskeleton was malformed. Thus, we conclude that talins are essential for kidney CD development via mechanisms that are both dependent and independent of their ability to bind to the β1 integrin subunit NPxY.

We have previously shown that deleting β1 integrin in the developing UB caused fatal hypoplastic dysplastic kidneys due to decreased UB branching morphogenesis and nephron formation

Development (2017) 144, 4148-4158 doi:10.1242/dev.149914

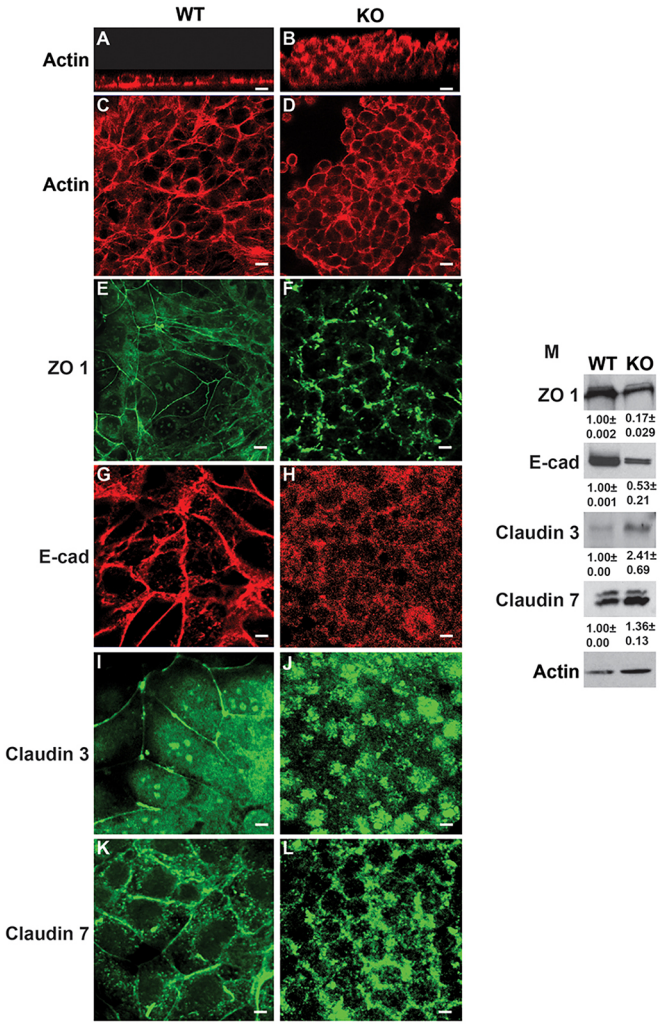

Fig. 9. Talin 1/2 KO CD cells have an integrin activation defect and altered expression of adherens and tight junction proteins. (A-L) Wild-type and talin 1/2 KO CD cells were grown on transwells until confluent in the presence of 10% FBS. The cells were then stained with rhodamine phalloidin (A-D) antibodies to ZO-1 (E,F), E-cadherin (E-cad) (G,H), claudin 3 (I,J) or claudin 7 (K,L). Scale bars: 100 µm. (M) Total cell lysates of wild-type and talin 1/2 KO CD cells were immunoblotted for ZO-1, E-cadherin (E-cad), claudin 3 or claudin 7. Densitometry results, which are shown below the blots, were normalized to the actin levels in the cells. This is representative of five experiments performed.

(Zhang et al., 2009). We later showed that YY/AA mutations in the membrane-proximal and -distal NPxY motifs caused both a moderately severe UB branching defect, intratubular cell proliferation and end-stage tubulointerstitial fibrosis of the kidney (Mathew et al., 2012b). The Y783A mutation described in this study results in a less serious phenotype than the YY/AA mutant with respect to intratubular cell proliferation and fibrosis, although the branching morphogenesis abnormalities are similar. We used the same *Hoxb7* cre mouse to delete β1 integrin and talins in this study as well as our two previous studies. This strategy helps justify the validity of our conclusion that the difference in the phenotypes is due to distinct functions of the β1 integrin or to deleting the talins. However, it must be borne in mind that hoxb7 Cre activity can be relatively chimeric for certain alleles throughout the ureteric epithelium (Marose et al., 2008; Yu et al., 2002; Zhao et al., 2004). Defects in the Y783A CD cells were also less severe than in the YY/AA CD cells, in every aspect examined (Mathew et al., 2012b). Thus, the membrane-proximal and -distal NPxY motifs differentially regulate UB development and CD cell function and signaling.

The progressively less severe effects of β1 integrin deletion, the YY/AA and the Y783A mutations in UB development, and CD cell tubulogenesis contrasts with other cell types. Integrin β1-null mice, as well as mice with β1 Y783A and YY/AA mutations constitutively knocked in, die at the pre-implantation stage (Meves et al., 2013), and their embryonic stem cells and fibroblasts have similar integrin activation and adhesion defects. By contrast, β1 Y783A expression in keratinocytes causes a milder phenotype than that observed in mice with either the β1 integrin gene deletion or the YY/AA substitutions (Meves et al., 2013). A Y/A mutation in the integrin β3 membrane proximal NPxY motif caused significantly less bleeding than that detected in integrin β3-null animals (Petrich et al., 2007b), although this mutation results in the absolute inability of integrin αIIbβ3 to bind fibrinogen (Petrich et al., 2007b).

The phenotype of the talin 1/2-null mice and CD cells was more severe than those detected in both the YY/AA (Mathew et al., 2012b) and β1 null (Zhang et al., 2009) mice and CD cells, suggesting that the defects caused by talin deletion are integrin β1 dependent and independent. Our data differ from mice where platelet talin 1 (the only talin expressed in platelets) was deleted (Nieswandt et al., 2007; Petrich et al., 2007b), or where mutations abrogating talin-β3 binding (Y747A and L746A corresponding to Y783A in the β1 subunit) were introduced (Petrich et al., 2007b). Fibrinogen-binding ability was affected equally in platelets from both sets of mice, although the bleeding phenotype was worse in the talin 1-null mice (Petrich et al., 2007a,b). A moderate adhesion and spreading defect was present in talin 1-null platelets on collagen 1, although platelet morphology was normal (Nieswandt et al., 2007; Petrich et al., 2007b). While the equivalent fibrinogen-binding defects in platelets from both the talin 1-null and Y747A and L746A mice were ascribed to abnormal talin 1-mediated β3 integrin function, the worse bleeding in the talin 1-null mice was proposed to be from altered activation/function of both β1 and β3 integrins. Another explanation proposed was that residual talin binding to integrin was still present despite the presence of disrupting mutations in the membrane proximal NPxY mutation (Nieswandt et al., 2007). It is possible the UB defect in the Y783A mice is less severe than the talin 1/2-null phenotype because it expresses other non-β1 integrins. However, no UB developmental abnormalities are described in integrin αv-null mice and the β1-null UB and CD phenotype (Zhang et al., 2009) was significantly less severe than in the talin 1/2 null mice and CD cells. Furthermore, our NMR data indicates an at least 50-fold reduction of affinity in the Y783A mutant, suggesting little binding is likely to occur under physiological conditions.

Our data suggest that the severe defect in UB development of the talin 1/2 null mouse is not due solely to its inability to activate integrins. This is consistent with studies where mice lacking talin 1 in podocytes died of kidney failure, and talin 1 depletion in podocytes caused a modest reduction in β1 integrin activation, podocyte adhesion and spreading that were accompanied by abnormalities in the actin cytoskeleton (Tian et al., 2014). Similarly, mice lacking both talin isoforms in muscle have a severe cardiomyopathy and die soon after birth, a defect that was not due to the inability of the muscle cells to activate integrins (Conti et al., 2008, 2009; Manso et al., 2013). Thus, unlike β3 integrins, which require talin for their activation and function, it appears that talin exerts many of its functions by mechanisms that are

Development (2017) 144, 4148-4158 doi:10.1242/dev.149914

independent of its requirement for integrin activation in the setting of β1 integrins.

When we explored alternative mechanisms whereby talins regulate CD cell function, we noted that talin 1/2 KO CD cells had a round morphology, were unable to form stress fibers, could not polarize, and had decreased expression and membrane localization of adherens junction proteins. These data suggest that strengthening of focal adhesions mediated by the talin rod plays a crucial role in regulating the actin cytoskeleton of CD cells (Albiges-Rizo et al., 2009; Atherton et al., 2015; Austen et al., 2015; Debrand et al., 2012; Meves et al., 2013). The mechanism whereby talins regulate adherens and tight junctions is currently unknown and worthy of further investigation. These data are consistent with the observations that: a proteolytic cleavage fragment of talin plays a major role in the formation of cadherin-mediated cell-cell adhesions (Zhang et al., 2012); the talin-binding protein vinculin helps maintain the interaction of β-catenin with MAGI-2, which is required to control PTEN protein expression (Subauste et al., 2005); and ZO-1 helps with the recruitment of actomyosin regulators, such as vinculin, which plays a role in endothelial barrier formation and cell-cell tension (Tornavaca et al., 2015). While the severe cytoskeleton alterations observed in the talin 1/2 null CD cells were similar to that of podocytes in which talin 1 was downregulated by siRNA (Tian et al., 2014), it contrasted with the persistent ability of these podocytes to adhere and spread. Our data also differ from the observations made in mammary epithelial cells where downregulation of talin 1 with siRNAs did not compromise β1 integrin activation, adhesion and spreading on multiple ECM substrates (Wang et al., 2011). These differences are likely because we deleted both talin isoforms genetically, while in the podocyte and mammary cell experiments, sufficient protein was still expressed for some talin-dependent functions.

In conclusion, this study shows that disrupting the principal talin-binding site of the β1 integrin in the UB of mice or CD cells resulted in a significantly less severe phenotype than simultaneous deletion of both talin genes. In addition to the severe integrin phenotype in the talin1/2 mice and cells, major phenotypical differences were seen in the actin cytoskeleton, cell polarity and expression of adherens and tight junction proteins. These results suggest that talins have major roles in cell function that are independent of the integrin β1-talin head interactions required for integrins to bind their ligands.

MATERIALS AND METHODS

Generation of mice

Experiments were approved by the Vanderbilt University Institutional Animal Use and Care Committee. Mice were an F7 to F10 generation toward the C57/Black6 background. The β1 integrin 783Y/A mouse was generated as previously described (Czuchra et al., 2006). These mice were intercrossed with floxed β1 integrin mice and hoxB7 promoter-driven Cre recombinase transgene mice (Yu et al., 2002). Talin-null mice in the UB were obtained by crossing talin $1^{flox/flox}$ mice with talin 2-null mice. These mice were then crossed with hoxB7-Cre mice.

Morphological and immunohistochemical analysis

Whole mouse embryos or kidneys were evaluated by light microscopy. Ki67 staining and scoring was performed as previously described (Mathew et al., 2012b). For whole-mount tissue visualization, intact kidney tissues were fixed in 4% PFA overnight and subjected to whole-mount immunofluorescent staining with primary antibody E-cadherin (Life Technologies, #131900) followed by incubation with Alexa anti-rat 568 IgG antibody. Images of kidneys in the same orientation were captured as *z*-stacks on a Nikon A1R confocal microscope. The raw confocal image was processed using ImageJ carrying the ND2 plug-in to create the 3D re-constructed image file and movie. The number of branch points per 3D re-constructed image of each mouse was counted. *In situ* hybridizations were performed as previously described (Marose et al., 2008).

Generation of integrin β1 cell lines

β1-null collecting-duct (CD) cells described previously (Zhang et al., 2009) were transfected with either full-length human integrin β1 (WT) or β1 integrins carrying the Y783A mutation. Equal surface expression of the β1 integrin subunits was obtained by flow cytometry sorting using the antibody AIIB2. The talin 1- and talin 2-null cells were isolated from the CDs of 5- to 6-week-old talin $1^{flox/flox}$ mice/talin 2-null mice and immortalized with pSV40 plasmid. The talin 1 gene was deleted with adenovirus expressing Cre recombinase. Multiple clones of the double null cells were prepared by performing serial dilution cloning and similar functionality was verified.

Cell adhesion, migration, proliferation and tubule formation

Laminin-511 was made as previously described (Yazlovitskaya et al., 2015) and rat tail collagen I was purchased from Sigma-Aldrich. Cell adhesion, migration and proliferation assays were performed as previously described (Chen et al., 2004). CD cells were grown in collagen/matrigel gels as previously described (Chen et al., 2004). The gels were stained with rhodamine-phalloidin and the tubules were photographed at 400× using a Zeiss Axio 510 confocal microscope.

Integrin activation assay

The active conformation of integrin β1 was determined using the conformation-specific antibody 12G10 (Millipore, MAB2247) for the human integrin β1 subunit and 9EG7 (BD Pharmingen, 555003) for the mouse integrin β1. The activation assays were carried out in the presence of 1.8 mM $CaCl_2$ and 1 mM $MgCl_2$ at room temperature. The amount of total antibody bound to the surface of cells was determined by flow cytometry. The total surface expression of integrin β1 was determined using AIIB2 antibody for human and anti-mouse integrin β1 antibody (BD Pharmingen, 550531) for the mouse integrin β1 subunit. The activation index is expressed as percentage of active conformation antibody binding relative to total surface expression of integrin β1.

Cell signaling

CD cells were serum starved for 12 h and plated on LM-511 (0.25 µg/ml), and harvested 0, 30, 45 and CD cells were seeded onto laminin 511-coated plates (0.25 µg/ml) in serum-free medium, allowed to attach for 1 h and serum starved for 12 h. Cells were exposed to GDNF or FGF10 for different time periods, and signaling was examined by immunoblotting with specific antibodies [pFAK (BD Bioscience 611807), FAK (Santacruz, sc-558), pAKT (Cell Signaling 9271), AKT (Cell Signaling 9272), pErk (Cell Signaling 9101), ERK (Cell Signaling 9102)].

Protein production

Protein purification of the integrin β1 TM/CTD domain and talin head (F0-F3) domain were carried out as described (Lu et al., 2016; Mathew et al., 2012b). Talin F0-F3 and the combined transmembrane and cytoplasmic (TM/CTD) domains of integrin β1 (719-798) were expressed with His_6 purification tags (N terminus for integrin β1 and C terminus for talin F0-F3). The bicelles were composed of q=0.3 D7PC/POPC/POPS, where q is the lipid (POPC +POPS)-to-detergent (D7PC) mole ratio. The POPC:POPS mole:mole ratio was 2:1. (POPC is 1-palmitoyl-2-oleoyl-phosphatidylcholine; POPS is 1-palmitoyl-2-oleoyl-phosphatidylserine). The precise methods for protein production are in the supplementary Materials and Methods.

Nuclear magnetic resonance spectroscopy

Peak assignments in the NMR spectrum of integrin β1 reported earlier (Lu et al., 2016; Mathew et al., 2012b) were used. NMR spectroscopy of the integrin β1 TM/CTD domain were carried out as described previously (Mathew et al., 2012b). NMR spectroscopy was carried out using a 900 MHz Bruker NMR spectrometer at 303 K. Uniformly labeled 15N-integrin β1 (0.2 mM) was titrated with unlabeled talin 1 head

Development (2017) 144, 4148-4158 doi:10.1242/dev.149914

domain (F0-F3, residues 1-433). The ^{1}H, ^{15N}-TROSY NMR spectrum of 0.2 mM ^{15}N-labeled integrin β1 was recorded and used as the first point of the titration experiment. Purified talin head (1-433, 500 µM stock also in bicelles) was then added to the NMR sample tube containing ^{15}N-labeled integrin β1 and then incubated for 2 h to allow complex formation prior to recording NMR spectrum. The intensities of selected residues were plotted against the total concentration of unlabeled talin head domain. Non-linear curve fitting was carried out using the program OriginPro9.0 using the following model for 1:1 binding. This model is general in that no assumption is made that the free ligand (i.e. talin head) equals the total ligand ($[L_0]$):

$$I_{obs} = (I_0 - I_s)\frac{(K_d + [L_0] + [P_0]) - \sqrt{(K_d + [L_0] + [P_0])^2 - (4[P_0][L_0])}}{2[P_0]} \quad (1)$$

where K_d is the dissociation constant, I_{obs} is the observed intensity, I_0 is the intensity of integrin β1 residue peak in the absence of talin, I_S the intensity at saturation with talin, P_0 is the total concentration of ^{15}N-labeled integrin β1 TM/CTD and L_0 is the total concentration of unlabeled talin head domain.

Detection of adherence and tight junction proteins

Immunofluorescence microscopy was performed on wild-type and talin 1/2 KO CD cells grown on transwells. The immunofluorescence was visualized using a Zeiss LSM 510 microscope. Immunoblotting of the junction proteins was carried out on whole cell lysates from cells grown on cell culture plates in the presence of 10% serum. Antibodies used for these studies are against E-cadherin (BD Bioscience 610181), ZO1 (Invitrogen 617330), claudin 3 (Invitrogen 341700) and claudin 7 (Sigma SAB4500437).

Statistics

Student's *t*-test was used for comparisons between two groups, and analysis of variance using Sigma Stat software was used for statistical differences between multiple groups. $P<0.05$ was considered statistically significant.

Competing interests

The authors declare no competing or financial interests.

Author contributions

Conceptualization: S.I., R.F., A.P., C.R.S., T.J.C., R.Z.; Methodology: S.M., R.J.P., G.M., Z.L., H.R., R.F., A.P., C.R.S., T.J.C., R.Z.; Formal analysis: R.Z.; Resources: D.R.C.; Data curation: S.M., G.M., Z.L., H.R., M.-Z.Z., C.R.S.; Writing - original draft: S.M., R.J.P., S.I., D.R.C., R.F., A.P., T.J.C., R.Z.; Writing - review & editing: S.M., D.R.C., R.F., A.P., C.R.S., R.Z.; Supervision: R.Z.

Funding

S.M. was funded by an American Heart Association Scientist Development grant (16SDG29740001). This work was funded by U.S. Department of Veterans Affairs Merit Review Awards (1I01BX002025 to A.P. and 1I01BX002196 to R.Z.) and by the National Institute of Diabetes and Digestive and Kidney Disease (R01-DK083187, R01-DK075594 and R01-DK069221 to R.Z., R01-DK095761 to A.P., and R01-DK080004, R01-DK095057 and R01-DK106743 to T.J.C.). Deposited in PMC for release after 12 months.

Supplementary information

Supplementary information available online at
http://dev.biologists.org/lookup/doi/10.1242/dev.149914.supplemental

References

Albiges-Rizo, C., Destaing, O., Fourcade, B., Planus, E. and Block, M. R. (2009). Actin machinery and mechanosensitivity in invadopodia, podosomes and focal adhesions. *J. Cell Sci.* **122**, 3037-3049.

Anthis, N. J., Wegener, K. L., Ye, F., Kim, C., Goult, B. T., Lowe, E. D., Vakonakis, I., Bate, N., Critchley, D. R., Ginsberg, M. H. et al. (2009). The structure of an integrin/talin complex reveals the basis of inside-out signal transduction. *EMBO J.* **28**, 3623-3632.

Anthis, N. J., Wegener, K. L., Critchley, D. R. and Campbell, I. D. (2010). Structural diversity in integrin/talin interactions. *Structure* **18**, 1654-1666.

Atherton, P., Stutchbury, B., Wang, D.-Y., Jethwa, D., Tsang, R., Meiler-Rodriguez, E., Wang, P., Bate, N., Zent, R., Barsukov, I. L. et al. (2015). Vinculin controls talin engagement with the actomyosin machinery. *Nat. Commun.* **6**, 10038.

Austen, K., Ringer, P., Mehlich, A., Chrostek-Grashoff, A., Kluger, C., Klingner, C., Sabass, B., Zent, R., Rief, M. and Grashoff, C. (2015). Extracellular rigidity sensing by talin isoform-specific mechanical linkages. *Nat. Cell Biol.* **17**, 1597-1606.

Bouaouina, M., Lad, Y. and Calderwood, D. A. (2008). The N-terminal domains of talin cooperate with the phosphotyrosine binding-like domain to activate beta1 and beta3 integrins. *J. Biol. Chem.* **283**, 6118-6125.

Calderwood, D. A., Zent, R., Grant, R., Rees, D. J. G., Hynes, R. O. and Ginsberg, M. H. (1999). The talin head domain binds to integrin beta subunit cytoplasmic tails and regulates integrin activation. *J. Biol. Chem.* **274**, 28071-28074.

Calderwood, D. A., Campbell, I. D. and Critchley, D. R. (2013). Talins and kindlins: partners in integrin-mediated adhesion. *Nat. Rev. Mol. Cell Biol.* **14**, 503-517.

Chen, D., Roberts, R., Pohl, M., Nigam, S., Kreidberg, J., Wang, Z., Heino, J., Ivaska, J., Coffa, S., Harris, R. C. et al. (2004). Differential expression of collagen- and laminin-binding integrins mediates ureteric bud and inner medullary collecting duct cell tubulogenesis. *Am. J. Physiol. Renal. Physiol.* **287**, F602-F611.

Conti, F. J., Felder, A., Monkley, S., Schwander, M., Wood, M. R., Lieber, R., Critchley, D. and Muller, U. (2008). Progressive myopathy and defects in the maintenance of myotendinous junctions in mice that lack talin 1 in skeletal muscle. *Development* **135**, 2043-2053.

Conti, F. J., Monkley, S. J., Wood, M. R., Critchley, D. R. and Muller, U. (2009). Talin 1 and 2 are required for myoblast fusion, sarcomere assembly and the maintenance of myotendinous junctions. *Development* **136**, 3597-3606.

Czuchra, A., Meyer, H., Legate, K. R., Brakebusch, C. and Fässler, R. (2006). Genetic analysis of beta1 integrin "activation motifs" in mice. *J. Cell Biol.* **174**, 889-899.

Debrand, E., Conti, F. J., Bate, N., Spence, L., Mazzeo, D., Pritchard, C. A., Monkley, S. J. and Critchley, D. R. (2012). Mice carrying a complete deletion of the talin2 coding sequence are viable and fertile. *Biochem. Biophys. Res. Commun.* **426**, 190-195.

Dressler, G. R. (2006). The cellular basis of kidney development. *Annu. Rev. Cell Dev. Biol.* **22**, 509-529.

Ginsberg, M. H. (2014). Integrin activation. *BMB Rep.* **47**, 655-659.

Goult, B. T., Bouaouina, M., Elliott, P. R., Bate, N., Patel, B., Gingras, A. R., Grossmann, J. G., Roberts, G. C. K., Calderwood, D. A., Critchley, D. R. et al. (2010). Structure of a double ubiquitin-like domain in the talin head: a role in integrin activation. *EMBO J.* **29**, 1069-1080.

Li, R., Babu, C. R., Lear, J. D., Wand, A. J., Bennett, J. S. and DeGrado, W. F. (2001). Oligomerization of the integrin alphaIIbbeta3: roles of the transmembrane and cytoplasmic domains. *Proc. Natl. Acad. Sci. USA* **98**, 12462-12467.

Lu, Z., Mathew, S., Chen, J., Hadziselimovic, A., Palamuttam, R., Hudson, B. G., Fassler, R., Pozzi, A., Sanders, C. R. and Zent, R. (2016). Implications of the differing roles of the beta1 and beta3 transmembrane and cytoplasmic domains for integrin function. *Elife* **5**.

Manso, A. M., Li, R., Monkley, S. J., Cruz, N. M., Ong, S., Lao, D. H., Koshman, Y. E., Gu, Y., Peterson, K. L., Chen, J. et al. (2013). Talin1 has unique expression versus talin 2 in the heart and modifies the hypertrophic response to pressure overload. *J. Biol. Chem.* **288**, 4252-4264.

Marose, T. D., Merkel, C. E., McMahon, A. P. and Carroll, T. J. (2008). Beta-catenin is necessary to keep cells of ureteric bud/Wolffian duct epithelium in a precursor state. *Dev. Biol.* **314**, 112-126.

Mathew, S., Chen, X., Pozzi, A. and Zent, R. (2012a). Integrins in renal development. *Pediatr. Nephrol.* **27**, 891-900.

Mathew, S., Lu, Z., Palamuttam, R. J., Mernaugh, G., Hadziselimovic, A., Chen, J., Bulus, N., Gewin, L. S., Voehler, M., Meves, A. et al. (2012b). beta1 integrin NPxY motifs regulate kidney collecting duct development and maintenanceby induced-fit interactions with cytosolic proteins. *Mol. Cell. Biol.* **32**, 4080-4091.

Meves, A., Geiger, T., Zanivan, S., DiGiovanni, J., Mann, M. and Fassler, R. (2011). Beta1 integrin cytoplasmic tyrosines promote skin tumorigenesis independent of their phosphorylation. *Proc. Natl. Acad. Sci. USA* **108**, 15213-15218.

Meves, A., Stremmel, C., Böttcher, R. T. and Fässler, R. (2013). beta1 integrins with individually disrupted cytoplasmic NPxY motifs are embryonic lethal but partially active in the epidermis. *J. Invest. Dermatol.* **133**, 2722-2731.

Monkley, S. J., Zhou, X.-H., Kinston, S. J., Giblett, S. M., Hemmings, L., Priddle, H., Brown, J. E., Pritchard, C. A., Critchley, D. R. and Fassler, R. (2000). Disruption of the talin gene arrests mouse development at the gastrulation stage. *Dev. Dyn.* **219**, 560-574.

Moore, D. T., Nygren, P., Jo, H., Boesze-Battaglia, K., Bennett, J. S. and DeGrado, W. F. (2012). Affinity of talin-1 for the beta3-integrin cytosolic domain is modulated by its phospholipid bilayer environment. *Proc. Natl. Acad. Sci. USA* **109**, 793-798.

Morse, E. M., Brahme, N. N. and Calderwood, D. A. (2014). Integrin cytoplasmic tail interactions. *Biochemistry* **53**, 810-820.

Development (2017) 144, 4148-4158 doi:10.1242/dev.149914

Moser, M., Legate, K. R., Zent, R. and Fassler, R. (2009). The tail of integrins, talin, and kindlins. *Science* **324**, 895-899.

Mould, A. P., Garratt, A. N., Askari, J. A., Akiyama, S. K. and Humphries, M. J. (1995). Identification of a novel anti-integrin monoclonal antibody that recognises a ligand-induced binding site epitope on the beta 1 subunit. *FEBS Lett.* **363**, 118-122.

Nieswandt, B., Moser, M., Pleines, I., Varga-Szabo, D., Monkley, S., Critchley, D. and Fässler, R. (2007). Loss of talin1 in platelets abrogates integrin activation, platelet aggregation, and thrombus formation in vitro and in vivo. *J. Exp. Med.* **204**, 3113-3118.

Petrich, B. G., Fogelstrand, P., Partridge, A. W., Yousefi, N., Ablooglu, A. J., Shattil, S. J. and Ginsberg, M. H. (2007a). The antithrombotic potential of selective blockade of talin-dependent integrin alpha IIb beta 3 (platelet GPIIb-IIIa) activation. *J. Clin. Invest.* **117**, 2250-2259.

Petrich, B. G., Marchese, P., Ruggeri, Z. M., Spiess, S., Weichert, R. A. M., Ye, F., Tiedt, R., Skoda, R. C., Monkley, S. J., Critchley, D. R. et al. (2007b). Talin is required for integrin-mediated platelet function in hemostasis and thrombosis. *J. Exp. Med.* **204**, 3103-3111.

Pozzi, A. and Zent, R. (2013). Integrins in kidney disease. *J. Am. Soc. Nephrol.* **24**, 1034-1039.

Praekelt, U., Kopp, P. M., Rehm, K., Linder, S., Bate, N., Patel, B., Debrand, E., Manso, A. M., Ross, R. S., Conti, F. et al. (2012). New isoform-specific monoclonal antibodies reveal different sub-cellular localisations for talin1 and talin2. *Eur. J. Cell Biol.* **91**, 180-191.

Saltel, F., Mortier, E., Hytönen, V. P., Jacquier, M.-C., Zimmermann, P., Vogel, V., Liu, W. and Wehrle-Haller, B. (2009). New PI(4,5)P2- and membrane proximal integrin-binding motifs in the talin head control beta3-integrin clustering. *J. Cell Biol.* **187**, 715-731.

Subauste, M. C., Nalbant, P., Adamson, E. D. and Hahn, K. M. (2005). Vinculin controls PTEN protein level by maintaining the interaction of the adherens junction protein beta-catenin with the scaffolding protein MAGI-2. *J. Biol. Chem.* **280**, 5676-5681.

Tian, X., Kim, J. J., Monkley, S. M., Gotoh, N., Nandez, R., Soda, K., Inoue, K., Balkin, D. M., Hassan, H., Son, S. H. et al. (2014). Podocyte-associated talin1 is critical for glomerular filtration barrier maintenance. *J. Clin. Invest.* **124**, 1098-1113.

Tornavaca, O., Chia, M., Dufton, N., Almagro, L. O., Conway, D. E., Randi, A. M., Schwartz, M. A., Matter, K. and Balda, M. S. (2015). ZO-1 controls endothelial adherens junctions, cell-cell tension, angiogenesis, and barrier formation. *J. Cell Biol.* **208**, 821-838.

Wang, P., Ballestrem, C. and Streuli, C. H. (2011). The C terminus of talin links integrins to cell cycle progression. *J. Cell Biol.* **195**, 499-513.

Wegener, K. L., Partridge, A. W., Han, J., Pickford, A. R., Liddington, R. C., Ginsberg, M. H. and Campbell, I. D. (2007). Structural basis of integrin activation by talin. *Cell* **128**, 171-182.

Wu, W., Kitamura, S., Truong, D. M., Rieg, T., Vallon, V., Sakurai, H., Bush, K. T., Vera, D. R., Ross, R. S. and Nigam, S. K. (2009). {beta}1-Integrin is required for kidney collecting duct morphogenesis and maintenance of renal function. *Am. J. Physiol. Renal. Physiol.* **297**, F210-F217.

Yazlovitskaya, E. M., Tseng, H.-Y., Viquez, O., Tu, T., Mernaugh, G., McKee, K. K., Riggins, K., Quaranta, V., Pathak, A., Carter, B. D. et al. (2015). Integrin alpha3beta1 regulates kidney collecting duct development via TRAF6-dependent K63-linked polyubiquitination of Akt. *Mol. Biol. Cell* **26**, 1857-1874.

Ye, F., Snider, A. K. and Ginsberg, M. H. (2014). Talin and kindlin: the one-two punch in integrin activation. *Front. Med.* **8**, 6-16.

Yu, J., Carroll, T. J. and McMahon, A. P. (2002). Sonic hedgehog regulates proliferation and differentiation of mesenchymal cells in the mouse metanephric kidney. *Development* **129**, 5301-5312.

Zhang, X., Mernaugh, G., Yang, D.-H., Gewin, L., Srichai, M. B., Harris, R. C., Iturregui, J. M., Nelson, R. D., Kohan, D. E., Abrahamson, D. et al. (2009). beta1 integrin is necessary for ureteric bud branching morphogenesis and maintenance of collecting duct structural integrity. *Development* **136**, 3357-3366.

Zhang, F., Saha, S. and Kashina, A. (2012). Arginylation-dependent regulation of a proteolytic product of talin is essential for cell-cell adhesion. *J. Cell Biol.* **197**, 819-836.

Zhao, H., Kegg, H., Grady, S., Truong, H.-T., Robinson, M. L., Baum, M. and Bates, C. M. (2004). Role of fibroblast growth factor receptors 1 and 2 in the ureteric bud. *Dev. Biol.* **276**, 403-415.